

Measurement of the WW production cross section with dilepton final states in $p\bar{p}$ collisions at $\sqrt{s} = 1.96$ TeV and limits on anomalous trilinear gauge couplings

V.M. Abazov³⁷, B. Abbott⁷⁵, M. Abolins⁶⁵, B.S. Acharya³⁰, M. Adams⁵¹, T. Adams⁴⁹, E. Aguilo⁶, M. Ahsan⁵⁹, G.D. Alexeev³⁷, G. Alkhalaf⁴¹, A. Alton^{64,a}, G. Alverson⁶³, G.A. Alves², L.S. Ancu³⁶, T. Andeen⁵³, M.S. Anzelc⁵³, M. Aoki⁵⁰, Y. Arnoud¹⁴, M. Arov⁶⁰, M. Arthaud¹⁸, A. Askew^{49,b}, B. Åsman⁴², O. Atramentov^{49,b}, C. Avila⁸, J. BackusMayes⁸², F. Badaud¹³, L. Bagby⁵⁰, B. Baldin⁵⁰, D.V. Bandurin⁵⁹, S. Banerjee³⁰, E. Barberis⁶³, A.-F. Barfuss¹⁵, P. Bargassa⁸⁰, P. Baringer⁵⁸, J. Barreto², J.F. Bartlett⁵⁰, U. Bassler¹⁸, D. Bauer⁴⁴, S. Beale⁶, A. Bean⁵⁸, M. Begalli³, M. Begel⁷³, C. Belanger-Champagne⁴², L. Bellantoni⁵⁰, A. Bellavance⁵⁰, J.A. Benitez⁶⁵, S.B. Beri²⁸, G. Bernardi¹⁷, R. Bernhard²³, I. Bertram⁴³, M. Besançon¹⁸, R. Beuselinck⁴⁴, V.A. Bezzubov⁴⁰, P.C. Bhat⁵⁰, V. Bhatnagar²⁸, G. Blazey⁵², S. Blessing⁴⁹, K. Bloom⁶⁷, A. Boehnlein⁵⁰, D. Boline⁶², T.A. Bolton⁵⁹, E.E. Boos³⁹, G. Borissov⁴³, T. Bose⁶², A. Brandt⁷⁸, R. Brock⁶⁵, G. Brooijmans⁷⁰, A. Bross⁵⁰, D. Brown¹⁹, X.B. Bu⁷, D. Buchholz⁵³, M. Buehler⁸¹, V. Buescher²², V. Bunichev³⁹, S. Burdin^{43,c}, T.H. Burnett⁸², C.P. Buszello⁴⁴, P. Calfayan²⁶, B. Calpas¹⁵, S. Calvet¹⁶, J. Cammin⁷¹, M.A. Carrasco-Lizarraga³⁴, E. Carrera⁴⁹, W. Carvalho³, B.C.K. Casey⁵⁰, H. Castilla-Valdez³⁴, S. Chakrabarti⁷², D. Chakraborty⁵², K.M. Chan⁵⁵, A. Chandra⁴⁸, E. Cheu⁴⁶, D.K. Cho⁶², S. Choi³³, B. Choudhary²⁹, T. Christoudias⁴⁴, S. Cihangir⁵⁰, D. Claes⁶⁷, J. Clutter⁵⁸, M. Cooke⁵⁰, W.E. Cooper⁵⁰, M. Corcoran⁸⁰, F. Couderc¹⁸, M.-C. Cousinou¹⁵, S. Crépe-Renaudin¹⁴, V. Cuplov⁵⁹, D. Cutts⁷⁷, M. Ćwiok³¹, A. Das⁴⁶, G. Davies⁴⁴, K. De⁷⁸, S.J. de Jong³⁶, E. De La Cruz-Burelo³⁴, K. DeVaughan⁶⁷, F. Déliot¹⁸, M. Demarteau⁵⁰, R. Demina⁷¹, D. Denisov⁵⁰, S.P. Denisov⁴⁰, S. Desai⁵⁰, H.T. Diehl⁵⁰, M. Diesburg⁵⁰, A. Dominguez⁶⁷, T. Dorland⁸², A. Dubey²⁹, L.V. Dudko³⁹, L. Dufflot¹⁶, D. Duggan⁴⁹, A. Duperrin¹⁵, S. Dutt²⁸, A. Dyshkant⁵², M. Eads⁶⁷, D. Edmunds⁶⁵, J. Ellison⁴⁸, V.D. Elvira⁵⁰, Y. Enari⁷⁷, S. Eno⁶¹, P. Ermolov^{39,†}, M. Escalier¹⁵, H. Evans⁵⁴, A. Evdokimov⁷³, V.N. Evdokimov⁴⁰, G. Facini⁶³, A.V. Ferapontov⁵⁹, T. Ferbel^{61,71}, F. Fiedler²⁵, F. Filthaut³⁶, W. Fisher⁵⁰, H.E. Fisk⁵⁰, M. Fortner⁵², H. Fox⁴³, S. Fu⁵⁰, S. Fuess⁵⁰, T. Gadfort⁷⁰, C.F. Galea³⁶, A. Garcia-Bellido⁷¹, V. Gavrilov³⁸, P. Gay¹³, W. Geist¹⁹, W. Geng^{15,65}, C.E. Gerber⁵¹, Y. Gershtein^{49,b}, D. Gillberg⁶, G. Ginther^{50,71}, B. Gómez⁸, A. Goussiou⁸², P.D. Grannis⁷², S. Greder¹⁹, H. Greenlee⁵⁰, Z.D. Greenwood⁶⁰, E.M. Gregores⁴, G. Grenier²⁰, Ph. Gris¹³, J.-F. Grivaz¹⁶, A. Grohsjean²⁶, S. Grünendahl⁵⁰, M.W. Grünewald³¹, F. Guo⁷², J. Guo⁷², G. Gutierrez⁵⁰, P. Gutierrez⁷⁵, A. Haas⁷⁰, N.J. Hadley⁶¹, P. Haefner²⁶, S. Hagopian⁴⁹, J. Haley⁶⁸, I. Hall⁶⁵, R.E. Hall⁴⁷, L. Han⁷, K. Harder⁴⁵, A. Harel⁷¹, J.M. Hauptman⁵⁷, J. Hays⁴⁴, T. Hebbeker²¹, D. Hedin⁵², J.G. Hegeman³⁵, A.P. Heinson⁴⁸, U. Heintz⁶², C. Hensel²⁴, I. Heredia-De La Cruz³⁴, K. Herner⁶⁴, G. Hesketh⁶³, M.D. Hildreth⁵⁵, R. Hirosky⁸¹, T. Hoang⁴⁹, J.D. Hobbs⁷², B. Hoeneisen¹², M. Hohlfeld²², S. Hossain⁷⁵, P. Houben³⁵, Y. Hu⁷², Z. Hubacek¹⁰, N. Huske¹⁷, V. Hynek¹⁰, I. Iashvili⁶⁹, R. Illingworth⁵⁰, A.S. Ito⁵⁰, S. Jabeen⁶², M. Jaffré¹⁶, S. Jain⁷⁵, K. Jakobs²³, D. Jamin¹⁵, C. Jarvis⁶¹, R. Jesik⁴⁴, K. Johns⁴⁶, C. Johnson⁷⁰, M. Johnson⁵⁰, D. Johnston⁶⁷, A. Jonckheere⁵⁰, P. Jonsson⁴⁴, A. Juste⁵⁰, E. Kajfasz¹⁵, D. Karmanov³⁹, P.A. Kasper⁵⁰, I. Katsanos⁶⁷, V. Kaushik⁷⁸, R. Kehoe⁷⁹, S. Kermiche¹⁵, N. Khalatyan⁵⁰, A. Khanov⁷⁶, A. Kharchilava⁶⁹, Y.N. Kharzheev³⁷, D. Khatidze⁷⁰, T.J. Kim³², M.H. Kirby⁵³, M. Kirsch²¹, B. Klima⁵⁰, J.M. Kohli²⁸, J.-P. Konrath²³, A.V. Kozelov⁴⁰, J. Kraus⁶⁵, T. Kuhl²⁵, A. Kumar⁶⁹, A. Kupco¹¹, T. Kurča²⁰, V.A. Kuzmin³⁹, J. Kvita⁹, F. Lacroix¹³, D. Lam⁵⁵, S. Lammers⁵⁴, G. Landsberg⁷⁷, P. Lebrun²⁰, W.M. Lee⁵⁰, A. Leflat³⁹, J. Lellouch¹⁷, J. Li^{78,‡}, L. Li⁴⁸, Q.Z. Li⁵⁰, S.M. Lietti⁵, J.K. Lim³², D. Lincoln⁵⁰, J. Linnemann⁶⁵, V.V. Lipaev⁴⁰, R. Lipton⁵⁰, Y. Liu⁷, Z. Liu⁶, A. Lobodenko⁴¹, M. Lokajicek¹¹, P. Love⁴³, H.J. Lubatti⁸², R. Luna-Garcia^{34,d}, A.L. Lyon⁵⁰, A.K.A. Maciel², D. Mackin⁸⁰, P. Mättig²⁷, A. Magerkurth⁶⁴, P.K. Mal⁸², H.B. Malbouisson³, S. Malik⁶⁷, V.L. Malyshev³⁷, Y. Maravin⁵⁹, B. Martin¹⁴, R. McCarthy⁷², C.L. McGivern⁵⁸, M.M. Meijer³⁶, A. Melnitchouk⁶⁶, L. Mendoza⁸, D. Menezes⁵², P.G. Mercadante⁵, M. Merkin³⁹, K.W. Merritt⁵⁰, A. Meyer²¹, J. Meyer²⁴, J. Mitrevski⁷⁰, R.K. Mommsen⁴⁵, N.K. Mondal³⁰, R.W. Moore⁶, T. Moulik⁵⁸, G.S. Muanza¹⁵, M. Mulhearn⁷⁰, O. Mundal²², L. Mundim³, E. Nagy¹⁵, M. Naimuddin⁵⁰, M. Narain⁷⁷, H.A. Neal⁶⁴, J.P. Negret⁸, P. Neustroev⁴¹, H. Nilsen²³, H. Nogima³, S.F. Novaes⁵, T. Nunnemann²⁶, G. Obrant⁴¹, C. Ochando¹⁶, D. Onoprienko⁵⁹, J. Orduna³⁴, N. Oshima⁵⁰, N. Osman⁴⁴, J. Osta⁵⁵, R. Otec¹⁰, G.J. Otero y Garzón¹, M. Owen⁴⁵, M. Padilla⁴⁸, P. Padley⁸⁰, M. Pangilinan⁷⁷, N. Parashar⁵⁶, S.-J. Park²⁴, S.K. Park³², J. Parsons⁷⁰, R. Partridge⁷⁷, N. Parua⁵⁴, A. Patwa⁷³, G. Pawloski⁸⁰, B. Penning²³, M. Perfilov³⁹, K. Peters⁴⁵, Y. Peters⁴⁵, P. Pétrouff¹⁶, R. Piegaia¹, J. Piper⁶⁵, M.-A. Pleier²², P.L.M. Podesta-Lerma^{34,e}, V.M. Podstavkov⁵⁰, Y. Pogorelov⁵⁵, M.-E. Pol², P. Polozov³⁸, A.V. Popov⁴⁰, C. Potter⁶, W.L. Prado da Silva³, S. Protopopescu⁷³, J. Qian⁶⁴, A. Quadt²⁴, B. Quinn⁶⁶, A. Rakitine⁴³,

M.S. Rangel¹⁶, K. Ranjan²⁹, P.N. Ratoff⁴³, P. Renkel⁷⁹, P. Rich⁴⁵, M. Rijssenbeek⁷², I. Ripp-Baudot¹⁹, F. Rizatdinova⁷⁶, S. Robinson⁴⁴, R.F. Rodrigues³, M. Rominsky⁷⁵, C. Royon¹⁸, P. Rubinov⁵⁰, R. Ruchti⁵⁵, G. Safronov³⁸, G. Sajot¹⁴, A. Sánchez-Hernández³⁴, M.P. Sanders¹⁷, B. Sanghi⁵⁰, G. Savage⁵⁰, L. Sawyer⁶⁰, T. Scanlon⁴⁴, D. Schaile²⁶, R.D. Schamberger⁷², Y. Scheglov⁴¹, H. Schellman⁵³, T. Schliephake²⁷, S. Schlobohm⁸², C. Schwanenberger⁴⁵, R. Schwienhorst⁶⁵, J. Sekaric⁴⁹, H. Severini⁷⁵, E. Shabalina²⁴, M. Shamim⁵⁹, V. Shary¹⁸, A.A. Shchukin⁴⁰, R.K. Shivpuri²⁹, V. Siccari¹⁹, V. Simak¹⁰, V. Sirotenko⁵⁰, P. Skubic⁷⁵, P. Slattery⁷¹, D. Smirnov⁵⁵, G.R. Snow⁶⁷, J. Snow⁷⁴, S. Snyder⁷³, S. Söldner-Rembold⁴⁵, L. Sonnenschein²¹, A. Sopczak⁴³, M. Sosebee⁷⁸, K. Soustruznik⁹, B. Spurlock⁷⁸, J. Stark¹⁴, V. Stolin³⁸, D.A. Stoyanova⁴⁰, J. Strandberg⁶⁴, S. Strandberg⁴², M.A. Strang⁶⁹, E. Strauss⁷², M. Strauss⁷⁵, R. Ströhmer²⁶, D. Strom⁵³, L. Stutte⁵⁰, S. Sumowidagdo⁴⁹, P. Svoisky³⁶, M. Takahashi⁴⁵, A. Tanasijczuk¹, W. Taylor⁶, B. Tiller²⁶, F. Tissandier¹³, M. Titov¹⁸, V.V. Tokmenin³⁷, I. Torchiani²³, D. Tsybychev⁷², B. Tuchming¹⁸, C. Tully⁶⁸, P.M. Tuts⁷⁰, R. Unalan⁶⁵, L. Uvarov⁴¹, S. Uvarov⁴¹, S. Uzunyan⁵², B. Vachon⁶, P.J. van den Berg³⁵, R. Van Kooten⁵⁴, W.M. van Leeuwen³⁵, N. Varelas⁵¹, E.W. Varnes⁴⁶, I.A. Vasilyev⁴⁰, P. Verdier²⁰, L.S. Vertogradov³⁷, M. Verzocchi⁵⁰, D. Vilanova¹⁸, P. Vint⁴⁴, P. Vokac¹⁰, M. Voutilainen^{67,f}, R. Wagner⁶⁸, H.D. Wahl⁴⁹, M.H.L.S. Wang⁷¹, J. Warchol⁵⁵, G. Watts⁸², M. Wayne⁵⁵, G. Weber²⁵, M. Weber^{50,g}, L. Welty-Rieger⁵⁴, A. Wenger^{23,h}, M. Wetstein⁶¹, A. White⁷⁸, D. Wicke²⁵, M.R.J. Williams⁴³, G.W. Wilson⁵⁸, S.J. Wimpenny⁴⁸, M. Wobisch⁶⁰, D.R. Wood⁶³, T.R. Wyatt⁴⁵, Y. Xie⁷⁷, C. Xu⁶⁴, S. Yacoub⁵³, R. Yamada⁵⁰, W.-C. Yang⁴⁵, T. Yasuda⁵⁰, Y.A. Yatsunenko³⁷, Z. Ye⁵⁰, H. Yin⁷, K. Yip⁷³, H.D. Yoo⁷⁷, S.W. Youn⁵³, J. Yu⁷⁸, C. Zeitnitz²⁷, S. Zelitch⁸¹, T. Zhao⁸², B. Zhou⁶⁴, J. Zhu⁷², M. Zielinski⁷¹, D. Zieminska⁵⁴, L. Zivkovic⁷⁰, V. Zutshi⁵², and E.G. Zverev³⁹

(The DØ Collaboration)

¹Universidad de Buenos Aires, Buenos Aires, Argentina

²LAFEX, Centro Brasileiro de Pesquisas Físicas, Rio de Janeiro, Brazil

³Universidade do Estado do Rio de Janeiro, Rio de Janeiro, Brazil

⁴Universidade Federal do ABC, Santo André, Brazil

⁵Instituto de Física Teórica, Universidade Estadual Paulista, São Paulo, Brazil

⁶University of Alberta, Edmonton, Alberta, Canada; Simon Fraser University, Burnaby, British Columbia, Canada; York University, Toronto, Ontario, Canada and McGill University, Montreal, Quebec, Canada

⁷University of Science and Technology of China, Hefei, People's Republic of China

⁸Universidad de los Andes, Bogotá, Colombia

⁹Center for Particle Physics, Charles University,

Faculty of Mathematics and Physics, Prague, Czech Republic

¹⁰Czech Technical University in Prague, Prague, Czech Republic

¹¹Center for Particle Physics, Institute of Physics, Academy of Sciences of the Czech Republic, Prague, Czech Republic

¹²Universidad San Francisco de Quito, Quito, Ecuador

¹³LPC, Université Blaise Pascal, CNRS/IN2P3, Clermont, France

¹⁴LPSC, Université Joseph Fourier Grenoble 1, CNRS/IN2P3,

Institut National Polytechnique de Grenoble, Grenoble, France

¹⁵CPPM, Aix-Marseille Université, CNRS/IN2P3, Marseille, France

¹⁶LAL, Université Paris-Sud, IN2P3/CNRS, Orsay, France

¹⁷LPNHE, IN2P3/CNRS, Universités Paris VI and VII, Paris, France

¹⁸CEA, Irfu, SPP, Saclay, France

¹⁹IPHC, Université de Strasbourg, CNRS/IN2P3, Strasbourg, France

²⁰IPNL, Université Lyon 1, CNRS/IN2P3, Villeurbanne, France and Université de Lyon, Lyon, France

²¹III. Physikalisches Institut A, RWTH Aachen University, Aachen, Germany

²²Physikalisches Institut, Universität Bonn, Bonn, Germany

²³Physikalisches Institut, Universität Freiburg, Freiburg, Germany

²⁴II. Physikalisches Institut, Georg-August-Universität Göttingen, Germany

²⁵Institut für Physik, Universität Mainz, Mainz, Germany

²⁶Ludwig-Maximilians-Universität München, München, Germany

²⁷Fachbereich Physik, University of Wuppertal, Wuppertal, Germany

²⁸Panjab University, Chandigarh, India

²⁹Delhi University, Delhi, India

³⁰Tata Institute of Fundamental Research, Mumbai, India

³¹University College Dublin, Dublin, Ireland

³²Korea Detector Laboratory, Korea University, Seoul, Korea

³³SungKyunKwan University, Suwon, Korea

- ³⁴ *CINVESTAV, Mexico City, Mexico*
- ³⁵ *FOM-Institute NIKHEF and University of Amsterdam/NIKHEF, Amsterdam, The Netherlands*
- ³⁶ *Radboud University Nijmegen/NIKHEF, Nijmegen, The Netherlands*
- ³⁷ *Joint Institute for Nuclear Research, Dubna, Russia*
- ³⁸ *Institute for Theoretical and Experimental Physics, Moscow, Russia*
- ³⁹ *Moscow State University, Moscow, Russia*
- ⁴⁰ *Institute for High Energy Physics, Protvino, Russia*
- ⁴¹ *Petersburg Nuclear Physics Institute, St. Petersburg, Russia*
- ⁴² *Stockholm University, Stockholm, Sweden, and Uppsala University, Uppsala, Sweden*
- ⁴³ *Lancaster University, Lancaster, United Kingdom*
- ⁴⁴ *Imperial College, London, United Kingdom*
- ⁴⁵ *University of Manchester, Manchester, United Kingdom*
- ⁴⁶ *University of Arizona, Tucson, Arizona 85721, USA*
- ⁴⁷ *California State University, Fresno, California 93740, USA*
- ⁴⁸ *University of California, Riverside, California 92521, USA*
- ⁴⁹ *Florida State University, Tallahassee, Florida 32306, USA*
- ⁵⁰ *Fermi National Accelerator Laboratory, Batavia, Illinois 60510, USA*
- ⁵¹ *University of Illinois at Chicago, Chicago, Illinois 60607, USA*
- ⁵² *Northern Illinois University, DeKalb, Illinois 60115, USA*
- ⁵³ *Northwestern University, Evanston, Illinois 60208, USA*
- ⁵⁴ *Indiana University, Bloomington, Indiana 47405, USA*
- ⁵⁵ *University of Notre Dame, Notre Dame, Indiana 46556, USA*
- ⁵⁶ *Purdue University Calumet, Hammond, Indiana 46323, USA*
- ⁵⁷ *Iowa State University, Ames, Iowa 50011, USA*
- ⁵⁸ *University of Kansas, Lawrence, Kansas 66045, USA*
- ⁵⁹ *Kansas State University, Manhattan, Kansas 66506, USA*
- ⁶⁰ *Louisiana Tech University, Ruston, Louisiana 71272, USA*
- ⁶¹ *University of Maryland, College Park, Maryland 20742, USA*
- ⁶² *Boston University, Boston, Massachusetts 02215, USA*
- ⁶³ *Northeastern University, Boston, Massachusetts 02115, USA*
- ⁶⁴ *University of Michigan, Ann Arbor, Michigan 48109, USA*
- ⁶⁵ *Michigan State University, East Lansing, Michigan 48824, USA*
- ⁶⁶ *University of Mississippi, University, Mississippi 38677, USA*
- ⁶⁷ *University of Nebraska, Lincoln, Nebraska 68588, USA*
- ⁶⁸ *Princeton University, Princeton, New Jersey 08544, USA*
- ⁶⁹ *State University of New York, Buffalo, New York 14260, USA*
- ⁷⁰ *Columbia University, New York, New York 10027, USA*
- ⁷¹ *University of Rochester, Rochester, New York 14627, USA*
- ⁷² *State University of New York, Stony Brook, New York 11794, USA*
- ⁷³ *Brookhaven National Laboratory, Upton, New York 11973, USA*
- ⁷⁴ *Langston University, Langston, Oklahoma 73050, USA*
- ⁷⁵ *University of Oklahoma, Norman, Oklahoma 73019, USA*
- ⁷⁶ *Oklahoma State University, Stillwater, Oklahoma 74078, USA*
- ⁷⁷ *Brown University, Providence, Rhode Island 02912, USA*
- ⁷⁸ *University of Texas, Arlington, Texas 76019, USA*
- ⁷⁹ *Southern Methodist University, Dallas, Texas 75275, USA*
- ⁸⁰ *Rice University, Houston, Texas 77005, USA*
- ⁸¹ *University of Virginia, Charlottesville, Virginia 22901, USA and*
- ⁸² *University of Washington, Seattle, Washington 98195, USA*

(Dated: April 3, 2009)

We provide the most precise measurement of the WW production cross section in $p\bar{p}$ collisions to date at a center of mass energy of 1.96 TeV, and set limits on the associated trilinear gauge couplings. The $WW \rightarrow \ell\nu\ell'\nu$ ($\ell, \ell' = e, \mu$) decay channels are analyzed in 1 fb⁻¹ of data collected by the D0 detector at the Fermilab Tevatron Collider. The measured cross section is $\sigma(p\bar{p} \rightarrow WW) = 11.5 \pm 2.1$ (stat + syst) ± 0.7 (lumi) pb. One- and two-dimensional 95% C.L. limits on trilinear gauge couplings are provided.

The non-Abelian gauge group structure of the electro-weak sector of the standard model (SM) predicts specific interactions between the γ , W , and Z bosons. Two vertices, $WW\gamma$ and WWZ , provide important contributions

to the $p\bar{p} \rightarrow WW$ production cross section. Understanding this process is imperative because it is an irreducible background to the most sensitive discovery channel for the Higgs boson at the Tevatron, $H \rightarrow WW$. A de-

tailed study of WW production also probes the triple gauge-boson couplings (TGCs), which are sensitive to low-energy manifestations of new physics from a higher mass scale, and is sensitive to the production and decay of new particles, such as the Higgs boson [1]. Studying WW production at the Fermilab Tevatron Collider provides an opportunity to explore constituent center of mass energies ($\sqrt{\hat{s}}$) higher than that available at the CERN e^+e^- Collider (LEP) [2], since SM WW production at the Tevatron has an average $\sqrt{\hat{s}} = 245$ GeV and a 57% probability for $\sqrt{\hat{s}} > 208$ GeV [1]. The Tevatron experiments have been active in studying the WW cross section and TGCs in the past [3, 4, 5]. In this Letter we present the most precise measurement of the WW production cross section in $p\bar{p}$ collisions to date and updated limits on anomalous $WW\gamma$ and WWZ couplings.

We examine WW production via the process $p\bar{p} \rightarrow W^+W^- \rightarrow \ell^+\nu\ell'^-\bar{\nu}$ ($\ell, \ell' = e, \mu$; allowing for $W \rightarrow \tau\nu \rightarrow \ell + n\nu$ decays) and use charged lepton transverse momentum (p_T) distributions to study the TGCs. The decay of two W bosons into electrons or muons results in a pair of isolated, high- p_T , oppositely charged leptons and a large amount of missing transverse energy (\cancel{E}_T) due to the escaping neutrinos. This analysis uses $p\bar{p}$ collisions at a center of mass energy of 1.96 TeV, as recorded by the D0 detector [6] at the Tevatron. A combination of single-electron (ee and $e\mu$ channels) or single-muon ($\mu\mu$ channel) triggers were used to collect the data, which correspond to integrated luminosities of 1104 (ee), 1072 ($e\mu$), and 1002 ($\mu\mu$) pb^{-1} [7].

Electrons are identified in the calorimeter by their electromagnetic showers, which must occur within $|\eta| < 1.1$ or $1.5 < |\eta| < 3.0$ [8]. In the ee channel, at least one electron must satisfy $|\eta| < 1.1$. Electron candidates must be spatially matched to a track from the central tracking system, isolated from other energetic particles, and have a shape consistent with that of an electromagnetic shower. Electron candidates must also satisfy a tight requirement on a multivariate electron discriminant which takes into account track quality, shower shape, calorimeter and track isolation, and E/p , where E is the calorimeter cluster energy and p is the track momentum. The p_T measurement of an electron is based on calorimeter energy information and track position.

Muons are reconstructed within $|\eta| < 2.0$, must be spatially matched to a track from the central tracking system, and are required to have matched sets of wire and scintillator hits before and after the muon toroid. The detector support structure limits the muon system coverage in the region $|\eta| < 1.1$ and $4.25 < \phi < 5.15$ [8]; in this region a single set of matched wire and scintillator hits is required. Additionally, muons must be isolated such that the p_T sum of other tracks in a cone $\mathcal{R} = \sqrt{(\Delta\eta)^2 + (\Delta\phi)^2} < 0.5$ is < 2.5 GeV and calorimeter energy within $0.1 < \mathcal{R} < 0.4$ is < 2.5 GeV.

The \cancel{E}_T is determined based on the calorimeter energy

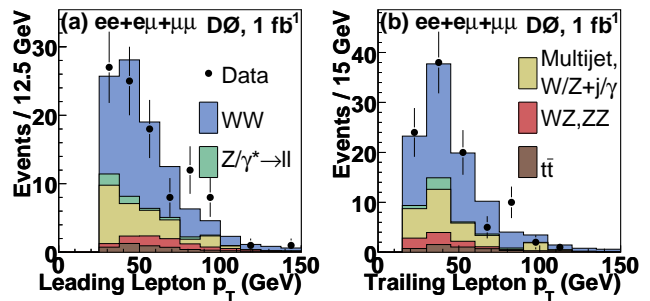


FIG. 1: Distributions of the (a) leading and (b) trailing lepton p_T after final selection, combined for all channels ($ee + e\mu + \mu\mu$). Data are compared to estimated signal, $\sigma(WW) = 12$ pb, and background sum.

deposition distribution with respect to the interaction vertex. It is corrected for the electromagnetic or jet energy scale, as appropriate, and the p_T of muons.

Signal acceptances and background processes are studied with a detailed Monte Carlo (MC) simulation based on PYTHIA [9] in conjunction with the CTEQ6L1 [10] parton distribution functions, with detector simulation carried out by GEANT [11]. The Z boson p_T spectrum in $Z/\gamma^* \rightarrow \ell\ell$ MC events is adjusted to match data [12].

For each final state, we require the highest p_T (leading) lepton to have $p_T > 25$ GeV, the trailing lepton to have $p_T > 15$ GeV, and the leptons to be of opposite charge. Both charged leptons are required to originate from the same vertex. The leptons must also have a minimum separation in η - ϕ space of $\mathcal{R}_{ee} > 0.8$ in the ee channel or $\mathcal{R}_{e\mu/\mu\mu} > 0.5$ in the $e\mu$ and $\mu\mu$ channels, in order to prevent overlap of the lepton isolation cones.

Background contributions to WW production from W +jets and multijet production are estimated from the data. Those from $Z/\gamma^* \rightarrow \ell\ell$, $t\bar{t}$, WZ , $W\gamma$, and ZZ are estimated from the MC simulation.

After the initial event selection, the dominant background in each channel is $Z/\gamma^* \rightarrow \ell\ell$ ($\ell = e, \mu, \tau$). Much of this background is removed by requiring $\cancel{E}_T > 45$ (ee), 20 ($e\mu$), or 35 ($\mu\mu$) GeV. For the ee channel, we require $\cancel{E}_T > 50$ GeV if $|M_Z - m_{ee}| < 6$ GeV to further reduce the $Z/\gamma^* \rightarrow \ell\ell$ background. In events containing muons, a requirement on the azimuthal separation ($\Delta\phi$) between the leptons is more effective at reducing the $Z/\gamma^* \rightarrow \ell\ell$ background than an invariant mass requirement, since the momentum resolution for high p_T muons is poorer than the calorimeter energy resolution for electrons. The $e\mu$ channel additionally requires $\cancel{E}_T > 40$ (instead of 20) GeV if $\Delta\phi_{e\mu} > 2.8$, and the $\mu\mu$ channel requires $\Delta\phi_{\mu\mu} < 2.45$.

Mismeasurement of the muon momentum can lead to spurious \cancel{E}_T which is collinear with the muon direction. Especially in the $\mu\mu$ channel, mismeasurement of the muon momentum can allow Z boson events to satisfy

the \cancel{E}_T requirement. To suppress these events in the $\mu\mu$ channel, we require that the track for each muon candidate include at least one silicon microstrip tracker hit, for better momentum resolution, and that the azimuthal angle between each muon and the direction of the \cancel{E}_T satisfies $|\cos(\Delta\phi_{\cancel{E}_T,\mu})| < 0.98$.

A second background is $t\bar{t}$ production followed by the leptonic decay of W bosons. This background can be suppressed by requiring $q_T = |\vec{p}_T^\ell + \vec{p}_T^{\ell'} + \vec{\cancel{E}}_T| < 20$ (ee), 25 ($e\mu$), or 16 ($\mu\mu$) GeV. This quantity is the p_T of the WW system and is expected to be small for signal events. However, for $t\bar{t}$ production and other background processes, q_T can be large, so this variable is a powerful discriminant against these backgrounds.

The $W\gamma$ process is a background for only the ee and $e\mu$ channels, since the probability for a photon to be misidentified as a muon is negligible. We determine the probability that a photon is misidentified as an electron with photons from $Z/\gamma^* \rightarrow ee\gamma$ decays and use it to correct the MC-based prediction of the $W\gamma$ background. The W +jets background, in which a jet is misidentified as an electron or muon, is determined from the data by selecting dilepton samples with loose and tight lepton requirements and setting up a system of linear equations to solve for the W +jet backgrounds after all event selection cuts, similar to the multijet background estimation performed in [13]. The multijet background contains jets that are misidentified as the two lepton candidates. It is represented by a data sample where the reconstructed leptons fail the lepton quality requirements. This sample is normalized with a factor determined at preselection using like-charged lepton events. It is assumed that misidentified jets result in randomly assigned charge signs.

The leptonic decay of WZ and ZZ events can mimic the WW signal when one or more of the charged leptons is not reconstructed and instead contributes to \cancel{E}_T . The $ZZ \rightarrow \ell\nu\ell'\nu$ process is suppressed by the $|M_Z - m_{ee}|$ or $\Delta\phi_{\ell\ell'}$ cut.

For each channel, the exact selection requirements on \cancel{E}_T , q_T , and $|M_Z - m_{ee}|$ or $\Delta\phi_{\ell\ell'}$ are chosen by performing a grid search on signal MC and expected background, minimizing the combined statistical and systematic uncertainty on the expected cross section measurement. The final lepton p_T distributions are shown in Fig. 1 [14].

The overall detection efficiency for signal events is determined using MC with full detector, trigger, and reconstruction simulation and is 7.18% (ee), 13.43% ($e\mu$), and 5.34% ($\mu\mu$) for $WW \rightarrow \ell\nu\ell'\nu$ ($\ell, \ell' = e, \mu$) decays and 2.24% (ee), 4.36% ($e\mu$), and 1.30% ($\mu\mu$) for $WW \rightarrow \tau\nu\ell\nu/\tau\nu\tau\nu \rightarrow \ell\ell' + n\nu$ decays. The numbers of estimated signal and background events and the number of observed events for each channel after the final event selection are summarized in Table I. The observed events

TABLE I: Numbers of signal and background events expected and number of events observed after the final event selection in each channel. Negligible contributions are not shown. Uncertainties include contributions from statistics and lepton selection efficiencies.

Process	ee	$e\mu$	$\mu\mu$
$Z/\gamma^* \rightarrow ee/\mu\mu$	0.27 ± 0.20	2.52 ± 0.56	0.76 ± 0.36
$Z/\gamma^* \rightarrow \tau\tau$	0.26 ± 0.05	3.67 ± 0.46	—
$t\bar{t}$	1.10 ± 0.10	3.79 ± 0.17	0.22 ± 0.04
WZ	1.42 ± 0.14	1.29 ± 0.14	0.97 ± 0.11
ZZ	1.70 ± 0.04	0.09 ± 0.01	0.84 ± 0.03
$W\gamma$	0.23 ± 0.16	5.21 ± 2.97	—
$W + \text{jet}$	6.09 ± 1.72	7.50 ± 1.83	0.12 ± 0.24
Multijet	0.01 ± 0.01	0.14 ± 0.13	—
$WW \rightarrow \ell\ell'$	10.98 ± 0.59	39.25 ± 0.81	7.18 ± 0.34
$WW \rightarrow \ell\tau/\tau\tau \rightarrow \ell\ell'$	1.40 ± 0.20	5.18 ± 0.29	0.71 ± 0.10
Total expected	23.46 ± 1.90	68.64 ± 3.88	10.79 ± 0.58
Data	22	64	14

are statistically consistent with the SM expectation in each channel. Assuming the W boson and τ branching ratios from [15], the observations in data correspond to $\sigma(p\bar{p} \rightarrow WW) = 10.6 \pm 4.6$ (stat) ± 1.9 (syst) ± 0.7 (lumi) pb in the ee channel, $10.8 \pm 2.2 \pm 1.1 \pm 0.7$ pb in the $e\mu$ channel, and $16.9 \pm 5.7 \pm 1.4 \pm 1.0$ pb in the $\mu\mu$ channel. The dominant sources of systematic uncertainty for each channel are the statistics associated with the estimation of the W +jet contribution in the ee channel, the photon misidentification probability used to estimate the $W\gamma$ contribution in the $e\mu$ channel, and the MC statistics for backgrounds in the $\mu\mu$ channel [14].

The cross section measurements in the individual channels are combined using the best linear unbiased estimator (BLUE) method [16] yielding: $\sigma(p\bar{p} \rightarrow WW) = 11.5 \pm 2.1$ (stat + syst) ± 0.7 (lumi) pb. The standard model calculation of the WW production cross section at the Tevatron center of mass energy is 12.0 ± 0.7 pb [17].

The TGCs that govern WW production can be parameterized by a general Lorentz-invariant Lagrangian with fourteen independent complex coupling parameters, seven each for the $WW\gamma$ and WWZ vertices [1]. Limits on the anomalous couplings are often obtained by taking the parameters to be real, enforcing electromagnetic gauge invariance, and assuming charge conjugation and parity invariance, reducing the number of independent couplings to five: g_1^Z , κ_Z , κ_γ , λ_Z , and λ_γ (using notation from [1]). In the SM, $g_1^Z = \kappa_Z = \kappa_\gamma = 1$ and $\lambda_Z = \lambda_\gamma = 0$. The couplings that are non-zero in the SM are often expressed in terms of their deviation from the SM values, e.g. $\Delta g_1^Z \equiv g_1^Z - 1$. Enforcing $SU(2)_L \otimes U(1)_Y$ symmetry introduces two relationships between the remaining parameters: $\kappa_Z = g_1^Z - (\kappa_\gamma - 1)\tan^2\theta_W$ and $\lambda_Z = \lambda_\gamma$, reducing the number of free parameters to

three [18]. Alternatively, enforcing equality between the $WW\gamma$ and WWZ vertices ($WW\gamma=WWZ$) such that $\kappa_\gamma = \kappa_Z$, $\lambda_\gamma = \lambda_Z$, and $g_1^Z = 1$ reduces the number of free parameters to two.

One effect of introducing anomalous coupling parameters into the SM Lagrangian is an enhancement of the cross section for the $q\bar{q} \rightarrow Z/\gamma^* \rightarrow W^+W^-$ process, which leads to unphysically large cross sections at high energy. Therefore, the anomalous couplings must vanish as the partonic center of mass energy $\sqrt{\hat{s}} \rightarrow \infty$. This is achieved by introducing a dipole form factor for an arbitrary coupling α (g_1^Z , κ_V , or λ_V): $\alpha(\hat{s}) = \alpha_0/(1+\hat{s}/\Lambda^2)^2$, where the form factor scale Λ is set by new physics, and limits are set in terms of α_0 . Unitarity constraints provide an upper limit for each coupling that is dependent on the choice of Λ . For this analysis we use $\Lambda = 2$ TeV, the approximate center of mass energy of the Tevatron.

The leading order MC event generator by Hagiwara, Woodside, and Zeppenfeld [1] is used to predict the changes in WW production cross section and kinematics as coupling parameters are varied about their SM values. At each point on a grid in TGC parameter space, events are generated and passed through a parameterized simulation of the D0 detector that is tuned to data. To enhance the sensitivity to anomalous couplings, events are sorted by lepton p_T into a two-dimensional histogram, using leading and trailing lepton p_T values in the ee and $\mu\mu$ channels, and e and μ p_T values in the $e\mu$ channel. For each bin in lepton p_T space, the expected number of WW events produced is parameterized by a quadratic function in three-dimensional $(\Delta\kappa_\gamma, \lambda_\gamma, \Delta g_1^Z)$ space or two-dimensional $(\Delta\kappa, \lambda)$ space, as appropriate for the TGC relationship scenario under study. In the three-dimensional case, coupling parameters are investigated in pairs, with the third parameter fixed to the SM value. A likelihood surface is generated by considering all channels simultaneously, integrating over the signal, background, and luminosity uncertainties with Gaussian distributions using the same methodology as that used in previous studies [5].

The one-dimensional 95% C.L. limits for $\Lambda = 2$ TeV are determined to be $-0.54 < \Delta\kappa_\gamma < 0.83$, $-0.14 < \lambda_\gamma = \lambda_Z < 0.18$, and $-0.14 < \Delta g_1^Z < 0.30$ under the $SU(2)_L \otimes U(1)_Y$ -conserving constraints, and $-0.12 < \Delta\kappa_\gamma = \Delta\kappa_Z < 0.35$, with the same λ limits as above, under the $WW\gamma=WWZ$ constraints. One- and two-dimensional 95% C.L. limits are shown in Fig. 2.

In summary, we have made the most precise measurement of WW production at a hadronic collider to date, $\sigma(p\bar{p} \rightarrow WW) = 11.5 \pm 2.1$ (stat + syst) ± 0.7 (lumi) pb, using 1 fb^{-1} of data at the D0 experiment. This result is consistent with the SM prediction and previous Tevatron results [3, 17, 19]. The selected event kinematics are used to significantly improve previous limits on anomalous TGCs from WW production at the Tevatron, reducing the allowed 95% C.L. interval for $\lambda_\gamma = \lambda_Z$ and

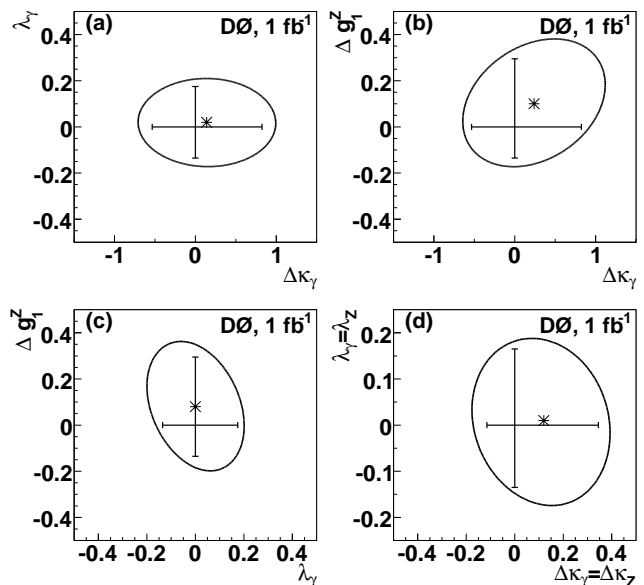


FIG. 2: One and two-dimensional 95% C.L. limits when enforcing $SU(2)_L \otimes U(1)_Y$ symmetry at $\Lambda = 2$ TeV, for (a) $\Delta\kappa_\gamma$ vs. λ_γ , (b) $\Delta\kappa_\gamma$ vs. Δg_1^Z , and (c) λ_γ vs. Δg_1^Z , each when the third free coupling is set to its SM value; limits when enforcing the $WW\gamma=WWZ$ constraints are shown in (d). The curve represents the two-dimensional 95% C.L. contour and the ticks along the axes represent the one-dimensional 95% C.L. limits. An asterisk (*) marks the point with the highest likelihood in the two-dimensional plane.

$\Delta\kappa_\gamma = \Delta\kappa_Z$ by nearly a factor of two [5, 20].

We thank the staffs at Fermilab and collaborating institutions, and acknowledge support from the DOE and NSF (USA); CEA and CNRS/IN2P3 (France); FASI, Rosatom and RFBR (Russia); CNPq, FAPERJ, FAPESP and FUNDUNESP (Brazil); DAE and DST (India); Colciencias (Colombia); CONACyT (Mexico); KRF and KOSEF (Korea); CONICET and UBACyT (Argentina); FOM (The Netherlands); STFC and the Royal Society (United Kingdom); MSMT and GACR (Czech Republic); CRC Program, CFI, NSERC and WestGrid Project (Canada); BMBF and DFG (Germany); SFI (Ireland); The Swedish Research Council (Sweden); CAS and CNSF (China); and the Alexander von Humboldt Foundation (Germany).

-
- [a] Visitor from Augustana College, Sioux Falls, SD, USA.
 - [b] Visitor from Rutgers University, Piscataway, NJ, USA.
 - [c] Visitor from The University of Liverpool, Liverpool, UK.
 - [d] Visitor from Centro de Investigacion en Computacion - IPN, Mexico City, Mexico.
 - [e] Visitor from ECFM, Universidad Autonoma de Sinaloa, Culiacán, Mexico.
 - [f] Visitor from Helsinki Institute of Physics, Helsinki, Fin-

land.

- [g] Visitor from Universität Bern, Bern, Switzerland.
- [h] Visitor from Universität Zürich, Zürich, Switzerland.
- [‡] Deceased.
- [1] K. Hagiwara, J. Woodside, and D. Zeppenfeld, Phys. Rev. D **41**, 2113 (1990); K. Hagiwara, R. D. Peccei, D. Zeppenfeld, Nucl. Phys. **B282**, 253 (1987).
- [2] S. Schael *et al.* (ALEPH Collaboration), Phys. Lett. B **614**, 7 (2005); P. Achard *et al.* (L3 Collaboration), Phys. Lett. B **586**, 151 (2004); G. Abbiendi *et al.* (OPAL Collaboration), Eur. Phys. J. C **33**, 463 (2004).
- [3] V. M. Abazov *et al.* (D0 Collaboration), Phys. Rev. Lett. **94**, 151801 (2005); V. M. Abazov *et al.* (D0 Collaboration), Phys. Rev. Lett. **100**, 139901(E) (2008).
- [4] D. Acosta *et al.* (CDF Collaboration), Phys. Rev. Lett., **94**, 211801 (2005).
- [5] V. M. Abazov *et al.* (D0 Collaboration), Phys. Rev. D **74**, 057101 (2006).
- [6] V. M. Abazov *et al.* (D0 Collaboration), Nucl. Instrum. Methods Phys. Res. A **565**, 463 (2006).
- [7] T. Andeen *et al.*, FERMILAB-TM-2365 (2007). A 6.1% uncertainty is assigned to the integrated luminosity measurement.
- [8] Pseudorapidity $\eta = -\ln[\tan(\frac{\theta}{2})]$, where θ is the polar angle as measured from the proton beam axis; ϕ is the azimuthal angle.
- [9] H. U. Bengtsson and T. Sjöstrand, Comput. Phys. Commun. **46**, 43 (1987); T. Sjöstrand *et al.*, Comp. Phys. Comm., **135**, 238 (2001). We use PYTHIA v6.319.
- [10] J. Pumplin *et al.*, J. High Energy Phys. **07**, 012 (2002).
- [11] R. Brun and F. Carminati, CERN Program Library Long Writeup W5013, 1993 (unpublished).
- [12] V. M. Abazov *et al.* (D0 Collaboration), Phys. Rev. Lett. **100**, 102002 (2008).
- [13] V. M. Abazov *et al.* (D0 Collaboration), Phys. Rev. D **74**, 112004 (2006).
- [14] See attached supplementary material.
- [15] C. Amsler *et al.*, Phys. Lett. B **667**, 1 (2008).
- [16] L. Lyons, D. Gibaut, and P. Clifford, Nucl. Instrum. Methods Phys. Res. A **270**, 110 (1988).
- [17] J. M. Campbell and R. K. Ellis, Phys. Rev. D **60**, 113006 (1999). Cross section calculated with the same parameters given in the paper, except with $\sqrt{s} = 1.96$ TeV.
- [18] A. De Rújula, M. B. Gavela, P. Hernandez and E. Masso, Nucl. Phys. **B384**, 3 (1992).
- [19] D. Acosta *et al.* (CDF Collaboration), Phys. Rev. Lett. **94**, 211801 (2005).
- [20] T. Aaltonen *et al.* (CDF Collaboration), Phys. Rev. D **76**, 111103 (2007).

SUPPLEMENTAL MATERIAL

The final lepton p_T distributions for individual analysis channels are shown in Figure 3. The uncertainty from each systematic source as a percentage of the final background estimate for each channel is provided in Table II.

In Table II, the “MC Statistics” uncertainty is based on the number of MC events used to estimate the number of background events after final selection. The “MC Cross Section” uncertainty is based on the PDF and scale uncertainties associated with the theoretical cross sections used to scale the MC-driven background estimations. The “MC Corrections” uncertainty accounts for data-driven reweighting of the MC that corrects for general event characteristics such as the primary vertex z -position and instantaneous luminosity distributions. The “ $\gamma \rightarrow e$ Mis-ID Rate” uncertainty is driven by statistics in the data sample used to determine that misidentification rate. Sources of systematic uncertainty for the

TABLE II: Uncertainty from each systematic source as a percentage of the final background estimate for each channel.

Systematic Source	ee	$e\mu$	$\mu\mu$
MC Statistics	2.6%	3.6%	12.8%
MC Cross Section	2.6%	2.2%	2.5%
MC Corrections	2.0%	6.1%	2.0%
Electron ID	0.3%	0.3%	—
Muon ID	—	0.4%	3.0%
$\gamma \rightarrow e$ Mis-ID Rate	1.2%	12.1%	—
W +jet Statistics	15.5%	7.5%	6.8%
W +jet e Efficiency & Mis-ID Rate	3.4%	2.9%	—
W +jet μ Efficiency & Mis-ID Rate	—	1.4%	2.1%
Total Background Uncertainty	16.4%	16.4%	15.3%

W +jet background estimation are separated into categories based upon their correlations across analysis channels. The “ W +jet Statistics” systematic is based on the number of events in data that pass a series of lepton identification requirements in each analysis channel, independently. The “ W +jet Lepton Efficiency & Mis-ID Rate” uncertainties are based on measuring the rate at which a lepton passes loose and tight identification in $Z/\gamma^* \rightarrow \ell\ell$ candidate events in data and the rate at which a jet is misidentified as a lepton with loose or tight identification based on dijet data.

The statistical uncertainty due to the number of observed events in each channel is the dominant source of final uncertainty.

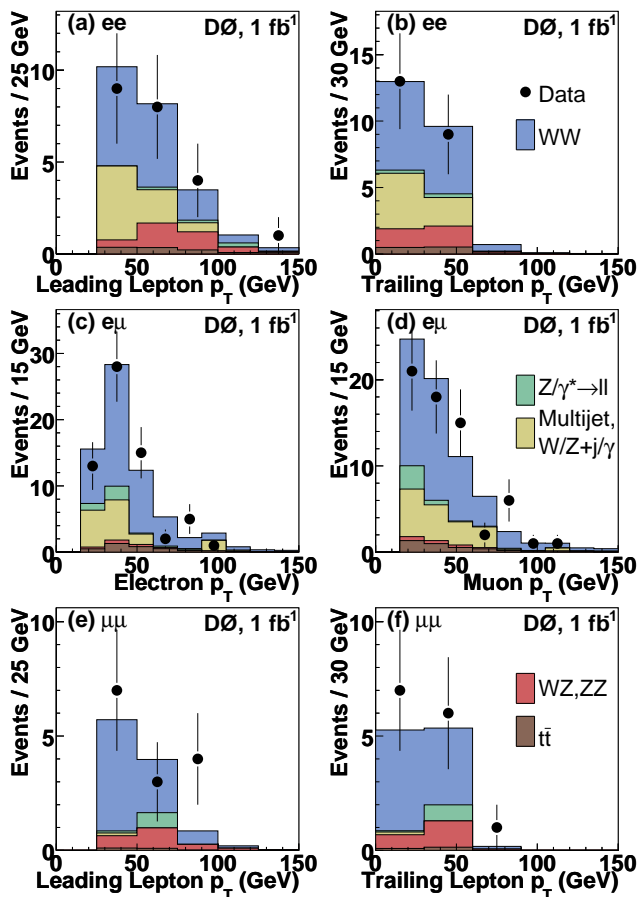


FIG. 3: Distributions of the (a) leading and (b) trailing electron p_T in the ee channel, (c) electron and (d) muon p_T in the $e\mu$ channel, and (e) leading and (f) trailing muon p_T in the $\mu\mu$ channel after final selection. Data are compared to estimated signal, $\sigma(WW) = 12$ pb, and background sum.